7

Single-pulse stimulation of cerebellar nuclei desynchronizes epileptic thalamus and cerebral cortex

Submitted to Current Biology:

O.H.J. Eelkman Rooda*, L. Kros*, S.J. Faneyte, P.J. Holland, S.V. Gornati, T.B. Houben, H.J. Poelman, N.A. Jansen, E.A. Tolner, A.M.J.M. van den Maagdenberg, C.I. De Zeeuw and F.E. Hoebeek

*These authors contributed equally

Experimental treatments for refractory epilepsy are currently remarkably diverse and range from no-invasive strategies like cannabidiol supplements and ketogenic diets to invasive deep brain stimulation. In the current era of optogenetic approaches and increasing understanding of neural networks, we revisited the first site that was used for neurostimulation in epilepsy patients, the cerebellum. Utilizing various electrophysiological and anatomical techniques, we addressed how controlling the cerebellar nuclei (CN) activity allows a highly effective control over generalized seizure activity in thalamocortical networks of the well-characterized CaV2.1 mutant mouse line tottering. Our multi-unit activity and single-unit recordings reveal that neuronal activity in thalamic nuclei, which is hypersynchronous during seizures, becomes desynchronized upon single-pulse optogenetic stimulation of CN neurons. We also found that throughout the thalamic complex CN stimulation results in a kaleidoscope of responses. We conclude that this cerebellar mediated desynchronization of thalamic activity is a crucial factor in the anti-epileptic effects of cerebellar stimulation and is well-worth further (clinical) investigation.

7.1 Introduction

Reorganization of local networks in the cerebral cortex following focal insults can facilitate the induction of more widespread hypersynchronized activity [423-427] and thereby lead to generalized seizures [428]. Directly restoring the activity of the cortical networks themselves forms a promising therapeutic strategy [97, 429], but manipulating the activity of upstream brain regions that provide prominent and specific synaptic inputs to these networks may be an interesting alternative. Here, we investigated how optogenetic stimulation of the cerebellar nuclei (CN) or their efferents affects the neuronal spiking patterns during seizures in the thalamus, which forms the major upstream hub of the cerebral cortex [97]. We show that single-pulse stimulation of CN neurons, which provide not only mono-synaptic but also multi-synaptic inputs to the thalamic nuclei [89, 430], is highly effective in stopping generalized absence seizures in tottering mice [46, 283] by instantly reducing synchronicity and rhythmicity in the thalamus. Notably, optogenetic stimulation of CN axons in the thalamic nuclei alone was less effective in stopping seizures than direct stimulation of CN neurons, supporting that the putative relevance of the upstream multi-synaptic cerebello-thalamic pathway is relevant. In between the seizures, thalamic responses to CN stimulation varied from short-latency increases to bimodal, inhibitory and delayed network effects. Our data show that single-pulse stimulation of CN neurons can stop epileptic seizures by desynchronizing thalamic neuronal firing, and they highlight the importance of cerebellar activity for controlling thalamo-cortical information processing in general.

7.2 Methods

Data were collected from male and female homozygous *tottering* mice (4- to 30-weeks-old) and their wild-type littermates, which were bred using heterozygous mice. The colony, originally purchased from Jackson laboratory (Bar Harbor, ME, USA), was maintained using C57BL/6NHsd mice obtained from Envigo laboratories (Horst, the Netherlands). PCR was used to confirm the presence of the tottering mutation in the *Cacna1a* gene using 5′-TTCTGGGTACCAGATACAGG-3′ (forward) and 5′-AAGTGTCGAAGTTGGTGCGC-3′ (reverse) primers (Eurogentech, Seraing, Belgium) and subsequent digestion using restriction enzyme *Nsb*I at the age of P9 - P12. All surgical and experimental procedures were performed in accordance with the European Communities Council Directive. Protocols were reviewed and approved by the institutional experimental animal committee (DEC).

7.2.1 Viral infection

Stereotactic viral injections were performed as previously described [46]. Briefly, the mice were kept under anesthesia in a custom made stereotactic frame. Craniotomies in the sagittal bone allowed us access to the cerebellar surface. We bilaterally injected virus-containing solutions (100 to 120 nL at a rate of ~20 nL/min) to transfect neurons in the interposed and lateral CN with Channelrhodopsin-2 (AAV2-hSyn-Chr2(H134R)-EYFP) [431]. After 10 minutes the injection pipette was slowly retracted and optic fibers were implanted ~200 μm above the injection site. Stereotaxic coordinates for CN injections were 2.5 mm posterior to lambda, 2.2 mm lateral to the midline and 2.2 mm below the pial surface. Viral vectors were originally designed by Dr. K. Deisseroth and were acquired from the University of North Carolina vector core.

7.2.2 Preparation for freely behaving recordings

Chronic electrode implantation was performed under isoflurane anesthesia (induction 4%; maintenance 1.5% in oxygen-enriched air) at the following coordinates (mm to bregma): -1.0 AP; +3.5 ML; -0.6 DV (right S1; single 75 μm platinum (Pt)/iridium (Ir) electrodes, PT6718; Advent Research Materials, Oxford, UK); or 1.0 mm AP; -1.5 mm ML; -0.6 mm V (right M1; single Pt/Ir electrodes) for LFP recordings; -1.3 mm AP; +1.25 mm ML; -3.1 mm DV (right VL; paired Pt/Ir); or -1.8 mm AP; +0.75 mm ML; -3.0 mm V (right CL; paired Pt/Ir); or -1.8 mm AP; +1.6 mm ML; -3.0 mm V (right VPL/VPM; paired Pt/Ir) for MUA recordings; two ball-tip electrodes (Ag, 75 μm) were positioned just posterior from lambda above cerebellum to serve as reference and ground electrodes. To enable optogenetic control of neuronal activity in CN, mice received 2 craniotomies in the interparietal bone for viral vector injection and placement of two optical fibers (200 μm diameter; CFML22L05, Thorlabs, Newton, NJ, USA) (-2.5 mm relative to lambda; 2.0 ML; 2.0 DV). CN were stereotactically injected bilaterally with 100-150 nl of the AAV2-hSyn-ChR2(H134R)-EYFP vector (kindly provided by Dr K. Deisseroth from Stanford University through the Vector Core at the University of North Carolina). Electrodes were connected to a 7-channel pedestal (E363/0 socket contacts and MS373 pedestal; Plastics One, Roanoke, VA, USA) and secured to the skull together with the optic fibers using light-activated bonding primer and dental cement (Kerr optibond / premise flowable, DiaDent Europe, Almere, the Netherlands) Carprofen (5 mg/kg, s.c.) and Temgesic (0.1 mg/kg, s.c.) was administered for post-operative pain relief.

7.2.3 Preparation for head-fixed in vivo recording

Male and female mice were anesthetized with a mixture of isoflurane (2% mixed with O_2. Body temperature was supported by a heating pad (FHC, Bowdoin, ME, USA). ECoG electrode implantation in M1 and S1 cortices was performed as previously described [46]. To enable extracellular recordings from thalamic neurons, a subset of mice received bilateral craniotomies (~ 1.5 mm diameter) in the parietal bone and great care was taken to preserve the dura mater. In another subset of mice the thalamic complex was implanted with optic fibers. These fibers were positioned using the following coordinates (in degrees (°) relative to the interaural axis and in mm relative to bregma): VL: 22° roll angle, -1.2 AP, -3.0 ML, -3.1 depth; VM: 2° roll angle, -1.2 AP, -1.1 ML, 3.3 depth; CL/CM: 0° roll angle, -1.3 AP, -0.75 ML, -3.0 depth; zona incerta: 0° roll angle, -2.5 AP, -1.75 ML, -3.6 depth). The positioning of the optic fibers was confirmed using immunofluorescent staining (see below). The exposed tissue was surrounded by a recording chamber, covered with tetracycline-containing ointment (Terra-cortril; Pfizer, New York, NY, USA) and sealed with silicon wax (Twinsil speed; Picodent, Wipperfurth, Germany). To allow the use of precise stereotactic coordinates during recording sessions we marked the position of bregma. After surgery, the mice recovered for at least five days in their home cage before experiments were performed.

7.2.4 *In vivo* extracellular electrophysiology

Following ~2-hour daily accommodation session in the setup on the first two days we performed recordings in awake, head-fixed mice on the third day lasting no longer than 4 hours. Although being head-fixed, the mice were able to move all limbs freely. The recording sessions typically were between 9:00 and 17:00, i.e., during the light period. Body temperature was supported using a heating pad (FHC). For extracellular single-unit recordings, custom-made, borosilicate glass capillaries (OD 1.5 mm, ID 0.86 mm; resistance 8–12 MΩ; taper length ~5 µm; tip diameter 0.5 µm) (Harvard Apparatus, Holliston, MA, USA) filled with 2 M NaCl were positioned stereotactically using an electronically driven pipette holder (SM7; Luigs & Neumann, Ratingen, Germany). Stereotactic coordinates for the thalamic recordings were tailored to the different thalamic nuclei. Thalamic neurons were localized by stereotactic location and a subset of recording sites was identified using iontophoretic injections of biocytin (1.5%, ~ 1 min, 4 sec on/off, 50% duty cycle, 4 µA), which was present in the NaCl-filled recording pipette.

ECoG recordings were filtered online using a 1–100 Hz band pass filter and a 50 Hz notch filter, sampled at 500 Hz and amplified before being stored for off-line analysis. Single-unit extracellular recordings were filtered online using a 30 Hz high pass filter and a 50 Hz notch

filter, sampled at 20 kHz and stored for off-line analysis. All electrophysiological recordings were performed using either a combination of CyberAmp 380 (Molecular Devices, LLC, Sunnyvale, Ca, USA), Neurodelta IR 183A or IR283A (Cygnus Technology Inc., Delaware Water Gap, PA, USA) and CED power 1401-3 (Cambridge England), or the combination of Multiclamp 700B and Digidata 1322A (Molecular Devices).

7.2.5 Optogenetics and electrophysiology in head-fixed *in vivo* preparation

For extracellular recordings combined with optogenetic CN or thalamic stimulation brief pulses (50 ms) of blue (470 nm) light were used to activate ChR2-infected CN neurons. Optic fibers (for CN stimulation: inner diameter = 200 μm, numerical aperture (NA) = 0.39; for thalamic stimulation: inner diameter = 105 μm, NA = 0.22; Thor Labs, Newton, NJ, USA) were placed ~200 μm from the injection site and connected to 470 nm LED sources (Thor Labs). Light intensity at the tip of the implantable fiber was 550 ± 50 μW/mm^2. We chose these optic fiber diameters following estimation of the light intensity in the brain so as to ensure that in CN sufficient neurons would be activated and that in thalamus a sufficient number of CN axons were activated. LEDs were activated for 50 ms at 0.2 Hz or by a closed-loop GSWD-detection system [46, 158].

7.2.6 Freely behaving electrophysiological recordings and optogenetic stimulation

After a 2-3 weeks recovery period, electrophysiological recordings were performed in freely behaving animals as described previously [432]. Electrophysiological signals were 3x pre-amplified and fed into separate ECoG (0.5-500 Hz, 800x gain) and MUA amplifiers (500-5,000 Hz; 12,000X gain). Signals were digitized (Power1401 and Spike2 software; CED) at 5,000 Hz (ECoG) or 25,000 Hz (MUA). Synchronized video-recordings made using a digital CCD camera at 30 frames/s (acA1300-60gmNIR; Basler, Ahrensburg, Germany). Optic fibers were connected to 470 nm LEDs (Thor Labs). Manual stimulation was performed to test efficacy of single pulse stimulation (0.5 mW/mm^2, 50 ms) for the disruption of GSWDs using a pulse generator (Prizmatix, Givat-Shmuel, Is) as previously described [46].

7.2.7 Pharmacological modulation of CN neurons

Procedure to increase CN action potential firing was performed as described previously [46]. Briefly, we located CN neurons after which we recorded one hour of 'baseline' ECoG. After this an injection was made with 100 μM gabazine ($GABA_A$-antagonist; Tocris)

dissolved in 1 M NaCl combined with fluorescence of Evans Blue (1% in 1 M NaCl) for histological verification. Next, we recorded during 20-50 min after the injection thalamic activity. The data on GSWD-occurrence following gabazine injection from 4 out of the 6 mice have been reported previously (**Fig. 2** in ref [46]).

7.2.8 Immunohistochemistry

Animals were anesthetized with pentobarbital (0.15 mL, intraperitoneal) immediately after acquiring the postinjection ECoG and perfused transcardially with saline followed by 4% paraformaldehyde (Sigma-Aldrich) in 0.1 M phosphate buffer (Sigma-Aldrich, pH = 7.4). Brains were removed and postfixed for 1–3 hours in 4% phosphate-buffered paraformaldehyde at room temperature, placed overnight in 10% sucrose in 0.1 M PB at 4°C and subsequently embedded in gelatine with 30% sucrose. We serially collected 50-µm-thick coronal sections for immunofluorescent staining. Cerebellar sections were incubated for 10 min with DAPI (300 nM) to verify the locations of viral injections and diencephalic sections were processed for parvalbumin staining (primary staining: 1:7,000 α-mouse, Swant #Pv-235; secondary staining: 1:200 mouse-α-donkey, Jackson Immunoresearch #715-175-150 (Westgrove, PA, USA) to locate thalamic nuclei and for biocytin staining to locate the recording sites. We confirmed the correct localization of the injections of gabazine and biocytin with images captured using a confocal laser scanning microscope (LSM 700; Zeiss, Lambrecht, Germany) at 555 nm (Evans Blue, Sigma), 488 (ChR2-EYFP) and 647 nm (parvalbumin).

7.2.9 Offline GSWD and extracellular action potential analysis

Both analysis of extracellular recordings and spontaneous GSWD characteristics were performed using previously described offline statistical analysis [46]. In brief, action potential analysis was performed using custom-written Matlab-based program SpikeTrain (Neurasmus, Erasmus MC Holding, Rotterdam, the Netherlands). Extracellular recordings were included if activity was stable and well isolated for at least 100 s. GSWD analysis was performed using a custom-written GSWD detection algorithm (LabVIEW, National Instruments, Austin, TX, USA). Co-efficient of variance (CV) was calculated as the ratio between the average and standard deviation of the interspike intervals (σ_{ISI}/μ_{ISI}), CV2 as $(2|ISI_{n+1} - ISI_n|/(ISI_{n+1} + ISI_n))$ [287] and burst index as (BI = number of action potentials within bursts / total number of action potentials) for which we defined 'burst' as a sequence of ≥3 spikes within 100 ms.

7.2.10 Offline MUA analysis

MUA data were analyzed using the template-matching method for spike sorting with an optimal spike threshold of 3 times SD from a 60-sec baseline recording. Sorted spikes were exported and analyzed following a custom-written algorithm in MATLAB to generate spike histograms. The spike-to-spike correlation (autocorrelation) was plotted based on a previous method [433]. Data points (x) were normalized (X_s) in a [0,1] range using the maximum spike count (x_{max}) and the minimum spike count (x_{min}): $X_s = x - x_{min} / x_{max} - x_{min}$. Mean correlation values were calculated by taking the ratio of the greatest correlation peak and the peak at t=0. The same time range was used to determine the greatest correlation in baseline and post-stimulation. Trials were included when the seizure ended 10 ms before stimulation and 150 ms after stimulation.

7.2.11 Assessment of modulation of TRN units

GSWD triggered rasterplots and peri-stimulus-time-histograms (PSTHs; 5 ms bin width) were used to calculate the modulation amplitude and frequency. ISIs of the data used for the rasterplots were subsequently shuffled randomly 500 times to create a normal distribution of modulation amplitudes. Cells were considered GSWD-modulated if the modulation amplitude was significantly higher than expected by chance, as indicated by a Z-score ($Z = (X-\mu)/\sigma$; $Z \geq 1.96$, $p \leq 0.05$) using the shuffled data as described previously [46], and if cells modulated at seizure frequency (6–9 Hz). The phase difference between the occurrence of the most negative deflection of a GSWD-episode and the time of the peak in thalamic activity was calculated by dividing this time difference by the median time difference between two GSWDs in that particular seizure.

7.2.12 Response of optogenetic stimulation

To determine if thalamic single units were significantly modulated following optogenetic CN stimulation we performed a random permutation calculation following a Monte-Carlo Bootstrap method, using 2 ms bin width PSTHs. For every recording we calculated the ISIs of action potentials 4 s prior to every pulse and combined them in a single ISI distribution, which was randomly permutated 250 times. We created PSTHs from these 'fake' spike times and calculated the average and standard deviation. If the PSTH of the 'true' spiking response to optogenetic stimuli breached the mean + 2SD threshold we noted the recording to have an increased firing response. For a subset of neurons we noticed a compelling inhibition. We marked the recording to have a decreased firing response if at any time during the post-stimulus period (5 s in total) 25 consecutive bins, i.e., 50 ms, the spike count was zero.

7.2.13 Assessment of fluorescence in thalamic nuclei

Guided by a reference atlas [434] we outlined the thalamic nuclei of interest. For each nucleus the expression pattern of ChR2-YFP was quantified with RGB measure function of Fiji (ImageJ) to calculate the mean intensity (in arbitrary units; a.u.) among the region of interest (ROI).

7.2.14 Interictal ECoG analysis

Analysis of EcoG data was performed with the fieldtrip toolbox (http://www.fieldtriptoolbox.org) in MATLAB. For the optogenetic data, stimuli that occurred during manually identified inter-ictal periods were extracted and subsequently any found to contain artefacts or short periods of increased oscillatory activity were removed from further analysis. Extracted epochs contained 4 s of activity both before and after the stimulus and data was bandpass filtered between 2 and 125 Hz prior to further analysis. Replacement of the stimulus artefact was performed by removing the section of data 700 ms prior to the stimulus to 300 ms after the stimulus and replacing it with a section of data extracted from 3 s prior to the stimulus on a trial by trial basis the ends of the replaced section were then smoothed to reduce edge effects. Spectrograms were calculated using Morlet wavelets with a width of 7 and evaluated at every sample.

For the Gabazine injection data, 100 epochs of 10 s were extracted from inter-ictal periods prior to injection (Baseline), immediately following injection (Early Post) and after ~1 hr (Late Post). Epochs with artefacts were rejected on the same basis as for the optogenetic data. The frequency content of the signals was calculated using Morlet Wavelets and normalized to the total power in the 2 to 115 Hz frequency band.

7.3 Statistical analysis

We examined the variance in each group using Kolmogorov-Smirnov and Shapiro-Wilk's test for normality. We analyzed the data using parametric (two-samples, one/two-tailed Student's *t*-test or (repeated measures) (M)ANOVA) or non-parametric (one/two-tailed Mann-Whitney U) depending on whether data was normally distributed. For the ECoG data statistical analysis of the power in each frequency band was carried out via repeated measures ANOVA with time point (Baseline, Early Post and Late Post) as the within-subject factor and recording location as the between subject factor. Only frequency bands which displayed a significant main effect of time point were subjected to post-hoc paired sample *t*-tests, Bonferroni-corrected *p*-values are reported in the figure legends. $P < 0.05$ is

considered significantly different. A single asterisk indicates $p < 0.05$, two asterisks indicate $p < 0.01$, three asterisks indicate $p < 0.001$.

7.4 Results

7.4.1 Cerebellar nuclei stimulation desynchronizes thalamic spiking activity

To examine the effects of CN stimulation on seizure-related thalamo-cortical neuronal activity patterns we recorded neuronal multi-unit activity (MUA) throughout the thalamic complex while monitoring cortical activity by ECoG in awake, freely behaving *tottering* mice (**Fig. 1A-C**). We observed that cortical generalized spike-and-wave discharges (GSWDs) were accompanied by rhythmic neuronal firing, i.e., characteristic for synchronized firing, in the thalamic complex. During interictal periods, however, thalamic MUA was relatively arrhythmic, i.e., characteristic for desynchronized firing (**Fig. 1C**).

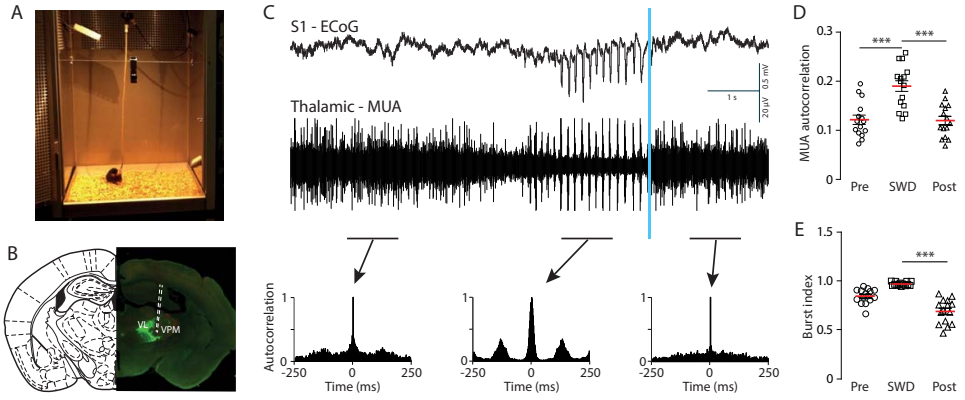

Figure 1. Single-pulse optogenetic CN stimulation stops rhythmic thalamic spiking.

(**A**) Tethered recording system for optogenetic stimulation in CN and thalamic neuronal multi-unit activity (MUA) and ECoG recordings from primary motor (M1) and sensory (S1) cortices in freely behaving *tottering* mice. (**B**) ChR2-EYFP-expressing CN axons in the thalamus complex with the location of the MUA electrode indicated by white-dashed lines. (**C**) (*Top - middle*) Example of spike-and-wave discharges (SWDs) in S1-ECoG (*top*) in synchrony with thalamic MUA (*middle*), during which mice developed behavioral arrest. Single-pulse optogenetic stimulation (vertical blue line; 50 ms, 470 nm, 0.5 mW/mm^2) in CN stopped synchronous burst firing in thalamic neurons and ended the SWDs, upon which behavioral arrest was typically ended. On average, SWDs occurred every 72.6 ± 19.8 s (N = 8 mice, 1-hour recording per mouse). (*Bottom*) Accompanying normalized autocorrelograms of MUA in 1-second periods of the pre-SWD, SWD and post-SWD phase. (**D**) Average MUA autocorrelation for pre-SWD, SWD and post-SWD multi-unit recordings. (**E**) As (D) but for burst index. Data are represented as mean ± SEM. * indicates $p < 0.05$, *** indicate $p < 0.001$ (see Online **Suppl. Table 1** for statistics).

Termination of seizure activity by optogenetic CN stimulation (single-pulse, 50 ms, 470 nm) (see also [46]) instantly reverted the phase-locked thalamic MUA to a desynchronized state, as shown by a reduction of the MUA autocorrelation (**Fig. 1C,D** and **Online Suppl. Table 1**). We also found that upon ictal CN stimulation the MUA burst index reverted to baseline levels (**Fig. 1E**). These findings indicate that single-pulse CN stimulation can consistently desynchronize seizure-related rhythmic thalamic MUA.

7.4.2 Thalamic responses to single-pulse cerebellar nuclei stimulation is variable

Our MUA recordings of thalamic neurons suggest that single-pulse stimulation in CN, which was shown to promote synchronous action potential firing [46], may have a differential effect on thalamic neurons. To further investigate the thalamic responses to CN stimulation, we recorded single-unit responses during interictal periods in head-fixed *tottering* mice (see STAR experimental procedures). Out of the 201 recorded neurons 165 neurons were responsive to single-pulse CN stimulation (50 ms pulse of 470 nm and 0.5 mW/mm^2 at 0.2 Hz) (**Fig. 2A**). Both the response latency and the type of response were variable (**Fig. 2B-D**) (see also **Suppl. Fig. 1** and **Online Suppl. Table 2**).

We observed a significant negative correlation between the pre-stimulus firing frequency and the number of spikes during the pulse (**Fig. 2C**). Most thalamic neurons increased their firing rate during CN stimulation (group 'increased'; 114 out of 165 neurons; 69.1%). Other thalamic neurons responded in a bi-phasic manner, i.e. following the initial excitatory response the firing rate was significantly reduced (group 'bi-phasic'; 17 out of 165; 10.3%). Again other thalamic neurons only showed a reduction of their firing rate upon CN stimulation (group 'decreased'; 15 out of 165; 9.1%). Finally we recorded neurons that did not show a significant response during the 50-ms stimulus, but only thereafter (group 'delayed'; 19 out of 165; 11.5%). Given that in a mouse brain the CN projection neurons that synapse onto thalamic neurons are known to be glutamatergic [245, 259], these recordings of bi-phasic-, decreased- and delayed-responses are most likely representing a combination of direct CN-input and additional afferent input possibly gated via CN-afferents to pre-thalamic nuclei [430]. To investigate the impact single-pulse CN stimulation has on cortical activity we analyzed M1 and S1 ECoG activities. As shown in the ECoG traces single-pulse CN stimulation resulted in a clear change of frequency and amplitude (**Fig. 2E,F**). A broadband decrease in power was observed lasting ~1 s; the most prominent suppression was found within in the seizure-related θ*-band (7-10 Hz) across the recording sites. We found that this response was reliably evoked, as can be seen from the averaged responses and power spectrogram (**Fig. 2G,H** and **Online Suppl. Table 3**).

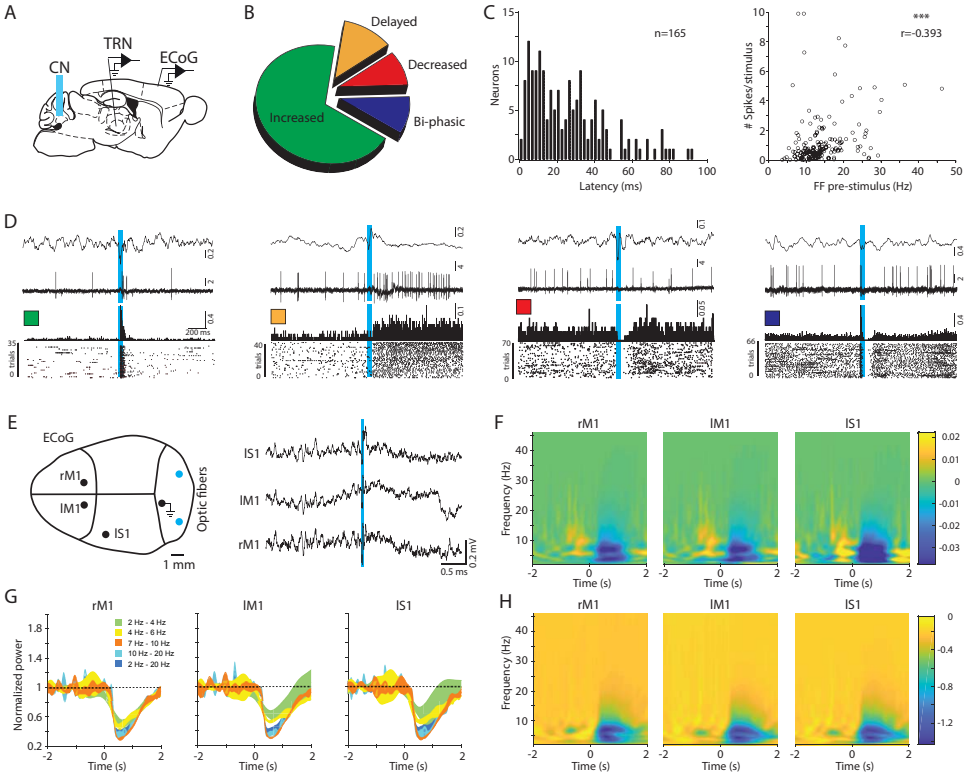

Figure 2. CN stimulation induces variable changes in interictal thalamic firing and cortical activity.

(**A**) Schematic outline of head-fixed experiment in *tottering* mice for CN optogenetic stimulation, single-unit extracellular recordings from thalamic relay neurons (TRN) and multi-site ECoG recordings from M1 and S1 regions. (**B**) Distribution of response types for the 165 thalamic neurons that showed a significant response to CN stimulation (as determined by Z-score based diagnostics; see STAR methods). See main text for number of cells per type of response. (**C**) (*Left*) Cumulative histogram of response latencies of thalamic neurons (n = 165 neurons) to single-pulse (50 ms) CN stimulation. (*Right*) Scatterplot for the correlation between the pre-stimulus firing frequency (FF) and the number of spikes recorded during the CN stimulus (Pearson's correlation coefficient: r = -0.393; $p < 0.001$). (**D**) Example traces of ECoG (*top traces*) and simultaneously recorded TRN (*bottom traces*) with accompanying per-stimulus histograms and scatterplots for each type of response. Green: 'increased' (see also **Suppl. Fig. 1B**); orange: 'delayed' (see also **Suppl. Fig. 1D**); red: 'decreased' (see also **Suppl. Fig. 1E**); and blue: 'bi-phasic' (see also **Suppl. Fig. 1C**). Vertical blue lines indicate time of optogenetic CN stimulation (50 ms). (**E**) (*Left)* Placement of craniotomies for ECoG recording electrodes and optic fibers in CN. (*Right*) Example ECoG trace from left S1 (lS1), left M1 (lM1) and right M1 (rM1) suggesting widespread effect of single-pulse optogenetic stimulation to bi-lateral CN (50 ms). (**F**) Normalized ECoG spectrogram from a single mouse (n = 246 stimuli) calculated following the masking of the large-amplitude ECoG response directly following the CN stimulation – to accurately analyze the post-stimulus response in all frequency bands (see STAR methods). This procedure is also applied to panels G and H. Note the clear drop in all frequency bands. (**G**) Normalized power in the separate frequency bands, indicating that in all recorded cortices a single-pulse CN stimulation resulted in a significant decrease in all channels, or in rM1 θ (4–7 Hz), θ* (7–10 Hz), β (10–20 Hz), and the broadband 2–20 Hz, but not in rM1 δ- (2–4 Hz) and γ (25–40 Hz) bands (N = 7 mice) (see Online **Suppl. Table 3** for statistics). (**H**) Normalized spectrogram accompanying panel G.

7.4.3 Pharmacological intervention of CN activity affects firing patterns of thalamic neurons

We previously showed that infusing $GABA_A$-receptor blocker gabazine (SR-95531) into the CN of *tottering* mice blocked GSWD occurrence and increased the frequency and regularity of CN spike firing [46]. To assess whether such long-term increases in CN firing had differential effects on interictal thalamic firing, as opposed to single-pulse CN stimulation, we recorded the effect of gabazine infusions into CN and found that the firing pattern of thalamic neurons was affected (**Suppl. Fig. 2A-C**). Comparison of the interictal activity recorded before and after gabazine infusion revealed that thalamic spiking contained less bursts and an increased level of regularity, while the average firing frequency was not significantly altered (**Suppl. Fig. 2D** and **Online Suppl. Table 4**). These alterations in thalamic firing indicate that upon gabazine infusion in CN, thalamic neurons shifted from the characteristic burst-pause firing pattern (related to a down-state of the membrane potential) to a more regular firing pattern (related to an up-state of the membrane potential) [99]. In parallel, the power of most ECoG frequency bands was changed (**Suppl. Fig. 2E-G**). Most notably, the power in the seizure-related θ*-band (7–10 Hz) was significantly decreased (**Suppl. Fig. 2H,I** and **Online Suppl. Table 5**). Together these data indicate that pharmacological interventions at the level of the CN affect the interictal firing pattern of thalamic neurons.

7.4.4 Factors contributing to the variability of thalamic responses to CN stimulation

Our current data indicate that single-pulse stimulation at a millisecond timescale and long-lasting pharmacological interventions, both of which increase CN firing [46], have a profound but variable effect on thalamic firing patterns and cortical network activity during interictal periods. This wide range of thalamic responses to optogenetic CN stimulation (**Fig. 2**) may have various causes. It may be that we recorded from different cell types [373]. Hereto we evaluated the firing pattern of thalamic neurons during GSWDs. We observed that 56.6% (69 out of 122 thalamic neurons) of the neurons revealed firing associated with GSWD patterns, i.e. 'GSWD-modulated' (**Fig. 3A-C**) (see also **Suppl. Fig. 3** and **Online Suppl. Table 6**), with a variable level of rhythmic spiking (**Fig. 3C**).

To assess whether the location of the recordings and thereby the afferent connections related to the rhythmic firing could contribute to the wide range of responses to CN stimulation we labelled the recording sites of 70 thalamic neurons (from 8 mice) using iontophoretic injections of biocytin (**Fig. 3D**).

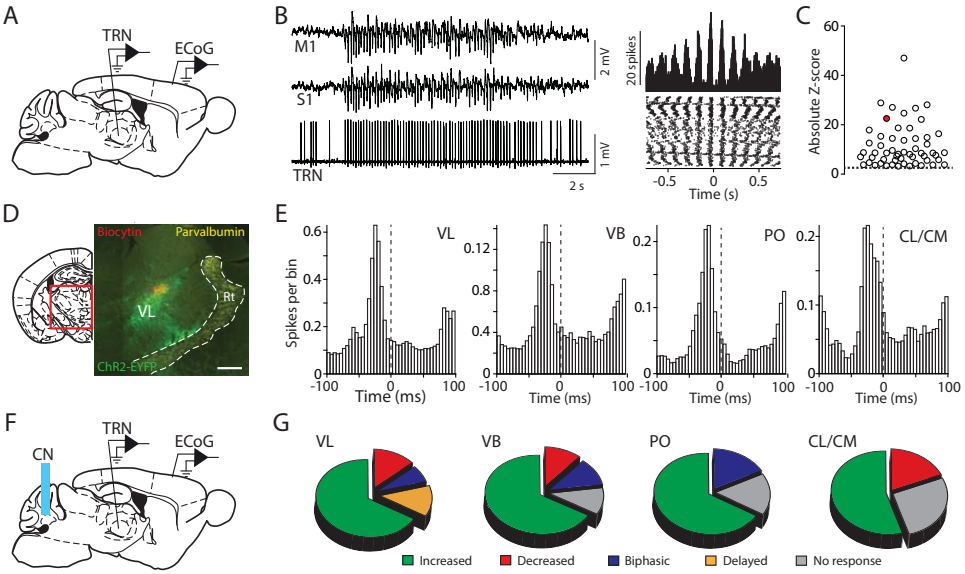

Figure 3. Varying thalamic responses to CN stimulation, but constant modulation by GSWDs.

(**A**) Schematic outline of head-fixed experiment for single-unit extracellular recordings from thalamic relay neurons (TRN) and multi-site ECoG recordings from M1 and S1 regions. (**B**) (*Left*) Typical example of TRN from which the firing becomes strongly associated with M1- and S1-recorded GSWDs. (*Right*) Accompanying per-ECoG-spike-histogram and scatterplot. (**C**) Absolute Z-score range for GSWD-modulated TRN recordings (Z-score = 9.97 ± 0.99; range 1.74 – 47.17; n = 69 cells from 8 mice). Note that all recordings (n = 53) with a Z-score < 1.96 are not represented in this panel for clarity of representation. The red circle indicates the neuron shown in (**B**). (**D**) Schematic and example image of immunohistological staining indicating the thalamic recording location (biocytin, red) in the VL nucleus that is innervated by ChR2-EYFP expressing CN axons (green). Reticular nucleus neurons are stained by parvalbumin (yellow). (**E**) Per-ECoG-spike histogram for all GSWD-modulated neurons recorded in VL (n = 15 cells; 7138 ECoG spikes from 3284 GSWD episodes), VB (n = 4 cells, 2064 ECoG spikes from 1369 GSWD episodes), PO (n = 5 cells, 2342 ECoG spikes from 1149 GSWDs) and CL/CM (n = 7 cells, 1645 ECoG spikes from 1066 GSWD episodes). Note that the time lag between histogram peaks only differs marginally (VL 23.1 ms, VB 16.0 ms, PO 16.2 ms, CL/CM 20.4 ms). (**F**) As (**A**) including optogenetic CN stimulation. (**G**) Proportions of neurons in VL (n = 20 neurons), VB (n = 9 neurons), PO (n = 6 neurons) and CL/CM (n = 11 neurons) that showed an 'increase', 'decrease', 'bi-phasic' or 'delayed' response upon single-pulse CN stimulation.

We found that a subpopulation of neurons throughout the various nuclei showed firing patterns directly associated with ECoG GSWDs. For these neurons the periodicity with the ECoG spikes was remarkably consistent per nucleus, ranging between 16.7 and 23.5 ms (**Fig. 3E**). In sharp contrast to these consistent firing patterns recording during ECoG GSWDs, we found that interictally the responses to single-pulse CN stimulation ranged widely throughout thalamic nuclei (**Fig. 3F**). In VL neurons we found that all recorded neurons changed their firing pattern upon CN stimulation. Most VL neurons increased the firing frequency, but the other response types (decreased, bi-phasic and delayed), which putatively can be linked to a multi-synaptic effect of CN stimulation, were also readily recorded (**Fig. 3G**).

Likewise, in the VB, PO and the intralaminar CL/CM nuclei we found several types of responses to CN firing, albeit that in these nuclei we also recorded several neurons the firing pattern of which did not change (**Fig. 3G**). These findings highlight not only that the various response types are not restricted to a particular thalamic nucleus, but also that throughout the various thalamic nuclei CN stimulation evokes a variety of changes in spiking patterns.

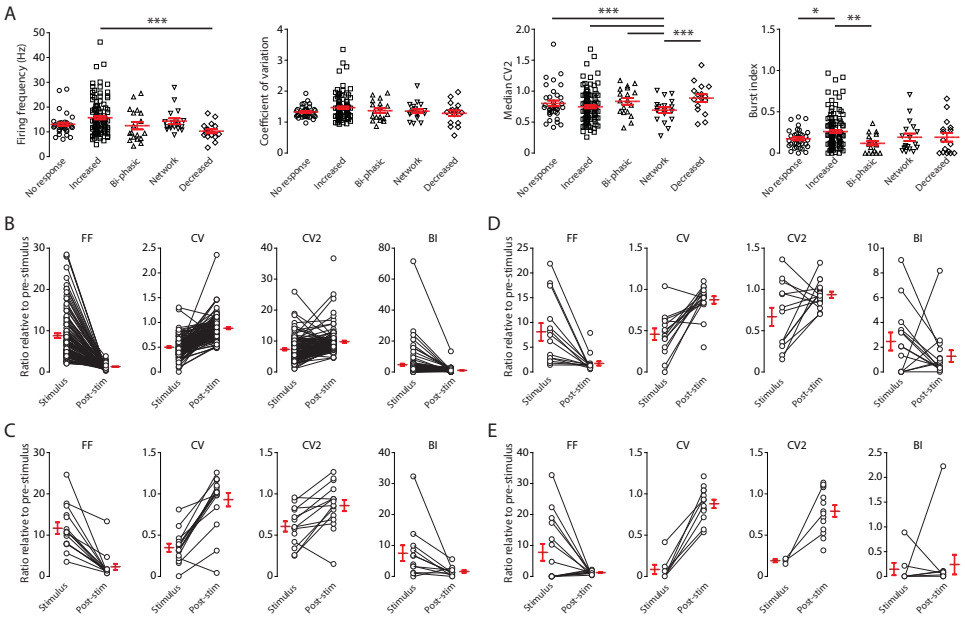

Supplemental Figure 1: Spiking pattern characteristics of thalamic relay neurons in relation to CN stimulation.

(**A**) Pre-stimulus firing frequency, coefficient of variation, median CV2 and burst index recorded from neurons that did not respond with a significantly altered spiking pattern to CN stimulation ('no response'; n = 36 neurons) and from neurons that responded with increased firing patterns during the 50-ms CN stimulation pulse ('increased'; n = 114 neurons), a bi-phasic modulation of spiking during the stimulus and post-stimulus period ('bi-phasic'; n = 17 neurons), a delayed response, i.e., no significant change in firing rate during the CN but only during the post-stimulus period ('delayed'; n = 15 neurons) or solely a decreased firing rate during the stimulus and/or post-stimulus periods ('decreased'; n = 19 neurons). See **Fig. 2D** for typical examples of each type of response. (**B**-**E**) Relative difference in firing frequency (FF), CV, CV2 and burst index (BI) during the stimulus and the post-stimulus period compared to the pre-stimulus period for all 'increased' (**B**), 'bi-phasic' (**C**), 'delayed' (**D**) and 'decreased' neurons (**E**). Only when the number of spikes allowed a calculation of all parameters the data points of the individual recordings are connected. Red markers indicate mean ± SEM. * indicates $p < 0.05$, ** $p < 0.01$ and *** $p < 0.001$. (see Online **Suppl. Table 2** for statistics).

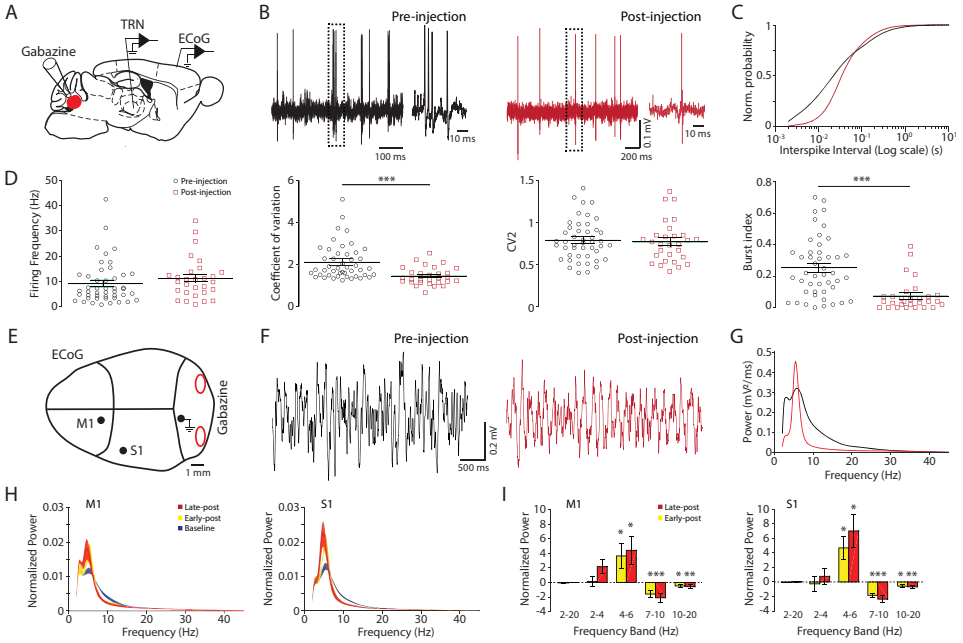

Supplemental Figure 2. Long-term modulation of cerebellar output by bilateral gabazine injections.

(**A**) Schematic outline of head-fixed experiment for CN injection of gabazine, single-unit extracellular recordings from thalamic relay neurons (TRN) and multi-site ECoG recordings from M1 and S1 regions. (**B**) Example traces of two single-unit TRNs: one in the absence (pre-injection; black) and one in the presence (post-injection; red) of gabazine in the bilateral CN. Note the presence (left trace) and absence (right) of burst-firing. (**C**) Normalized cumulative distribution for the interspike interval of thalamic neurons pre-injection (black) and post-injection of gabazine in the bilateral CN. (**D**) Average firing frequency, coefficient of variation (CV), CV2 and burst-index calculated for neurons recorded pre-gabazine (n = 46 neurons, N = 4 mice) and another set of neurons post-gabazine (n = 29 neurons, N = 4 mice). ** indicate $p < 0.01$. (**E**) Placement of craniotomies for ECoG recording electrodes and gabazine injections into the CN. (**F**) Four seconds of M1 ECoG recording pre-gabazine (*left*, black) and post-gabazine (*right*, red) from a single mouse. (**G**) Result of fast-Fourier transform of pre-gabazine (black) and post-gabazine (red) M1 ECoG. (**H**) Normalized ECoG power in M1 (*left*) and S1 (*right*) recordings from 4 mice, comparing pre-gabazine (baseline), ~5–20 min after gabazine (early-post) and ~1 hour after gabazine (late-post). (**I**) Relative change in ECoG power (normalized to pre-gabazine condition) showing an increase in θ- (4–7 Hz) power and a significant decrease in the β-band (10–20 Hz) and the θ*-band (7–10 Hz). The power in δ- (2–4 Hz), γ (25–40 Hz) and broadband 2–20 Hz activity was not affected. Note that there was no difference between M1 and S1 responses (see also [68]). * indicates $p < 0.05$, ** indicate $p < 0.01$ and ** indicate $p < 0.001$. See Online **Suppl. Tables 4 and 5** for statistics.

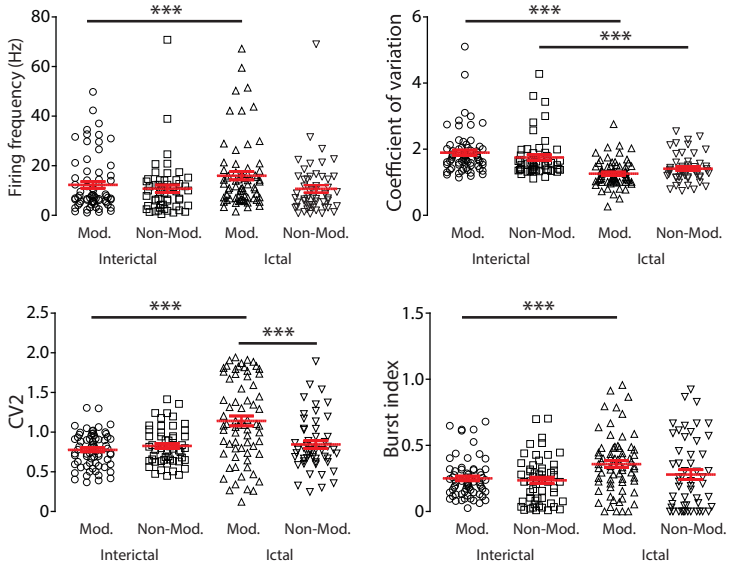

Supplemental Figure 3: Spiking pattern characteristics of thalamic relay neurons in relation to ECoG spike-and-wave discharges.

Firing frequency, coefficient of variation, CV2 and burst index for thalamic relay neurons that revealed spike-and-wave discharge (GSWD)-modulated or non-modulated spiking. Each firing parameter is represented for the interictal and ictal phases (determined by the occurrence of SWDs; see STAR methods section). Red markers indicate mean ± SEM. *** indicate $p < 0.001$ (see Online **Suppl. Table 6** for statistics).

7.4.5 CN neuron stimulation is more effective than activation of cerebellar efferents inside thalamus

To determine whether controlling the activity of a portion of CN axonal input to thalamic neurons is sufficient to stop GSWDs, we implanted optic fibers directly in nuclei of the thalamic complex. We initially focused on VL and VM since the density of CN axons, as evidence by the level of fluorescence from AAV-ChR2-EYFP transfected CN axons, in these nuclei was highest (VL: 47.5 ± 11.2 a.u.; VM: 54.5 ± 14.0 a.u.; N = 5 mice) (see also [435]). Given that VL and VM not only innervate M1, but also prefrontal, sensory and associative cortical regions [367, 368], we reasoned that stimulating only the CN axons in these nuclei may be sufficient to stop the widespread cortical oscillations underlying absence seizures. To test this premise, we implanted optic fibers bilaterally in VL and VM and ensured that the level of light intensity was sufficient to in principle activate ChR2-expressing CN axons throughout the thalamic nuclei (see STAR Methods). Surprisingly, optogenetic stimulation of these regions stopped only a proportion of seizures, regardless of whether we stimulated uni- or bilaterally (**Fig. 4A-C**).

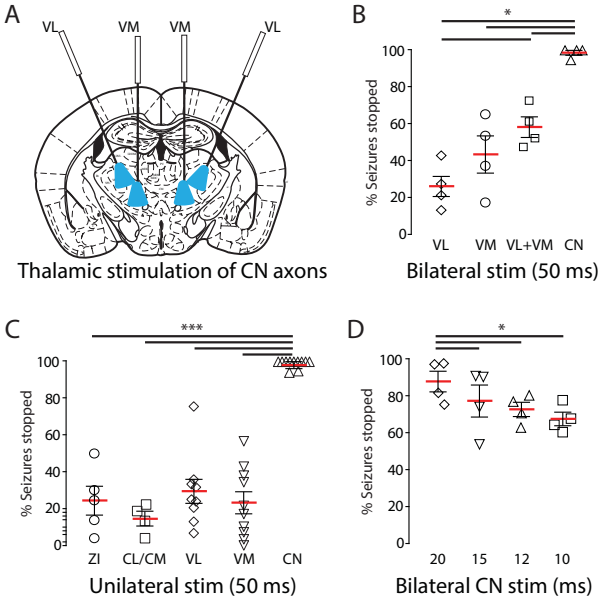

Figure 4. Activation of cerebellar afferents in thalamic nuclei is less sufficient in stopping GSWDs compared with direct cerebellar nuclei neuron stimulation.

(**A**) Experimental setup with four optic fibers implanted in thalamic nuclei. (**B**) Proportion of the seizures that stopped following bilateral VL (bilateral VL 25.8 ± 1.8% N = 4 animals; 244 seizures), bilateral VM (56.2 ± 6.0% N = 4 animals; 185 seizures), quadruple VL/VM (57.3 ± 3.9%, N = 4 mice, 250 seizures) or bilateral CN stimulation (98.7 ± 1.3% N = 4 animals; 3,254 seizures). (**C**) Proportion of the seizures that stopped following unilateral zona incerta (ZI) (24.4 ± 7.8 %; N = 5 sites; 302 seizures), CL/CM (16.8 ± 2.2 %, N = 4 animals; 205 seizures), VL (31.7 ± 2.7 %, N = 5 mice, 281 seizures), VM (32.9 ± 5.0%, N = 6 mice, n = 417 seizures) or CN stimulation (98.0 ± 1.9%, N = 11 sites; 199 seizures). (**D**) Proportion of the seizures that stopped following bilateral CN stimulation with varying pulse lengths. Data from the same mice as reported in B. Note that at 10-ms pulse length, CN stimulation is still effective in stopping most seizures. Data are represented as mean ± SEM. * indicates $p < 0.05$, *** indicate $p < 0.001$ (see Online Suppl. Table 7 for statistics).

In an attempt to increase the efficacy of seizure termination we activated all thalamic optic fibers simultaneously, but 50-ms pulses applied bilaterally to both VL and VM still only stopped a proportion of seizures (**Fig. 4B** and **Online Suppl. Table 7**). In the same mice, we also implanted optic fibers in the CN. In contrast to VL/VM stimulation bilateral CN stimulation stopped nearly all seizures (98.7 ± 1.3%); significantly more than in any of the VL/VM stimulation conditions. Even when we decreased the pulse length to 10 ms the efficacy of stopping GSWDs by direct CN stimulation (71.4 ± 6.8%) was at least as effective as applying 50 ms pulses to the VL and VM optic fibers simultaneously (**Fig. 4D** and **Online Suppl. Table 7**). To evaluate whether selective activation of CN axons in other thalamic nuclei is more effective in stopping seizures, we also implanted fibers in the zona incerta and in the intralaminar CL and CM nuclei, for which unilateral electrical or optogenetic stimulation was

shown to dampen cortical seizure activity [60, 436]. However, neither unilateral stimulation of CN terminals in zona incerta nor in CL/CM was as effective as unilateral stimulation of CN neurons (**Fig. 4C** and **Online Suppl. Table 7**). Collectively these data reveal that direct optogenetic CN stimulation has a more reliable effect in GSWD termination than activating proportions of cerebellar axons throughout the thalamic complex.

7.5 Discussion

Using a combination of *in vivo* electrophysiological and optogenetic techniques we could show that single-pulse stimulation of CN has a varying effect on neuronal spiking patterns throughout the thalamic complex, causing desynchronization of thalamic activity that disrupts epileptogenic GSWDs. Controlling the activity in CN for a fraction of a second was sufficient to desynchronize thalamic neurons for a prolonged period of time. Thereby our findings unveil a previously unknown function of cerebellar output in potentially directly affecting information processing in thalamo-cortical networks. We suggest that both under healthy and pathological conditions CN firing can direct the extent of thalamic synchronization and thereby contribute to neuronal network patterns encoded in various cerebral regions.

In freely behaving *tottering* mice thalamic neuronal activity recordings showed phase-locked action potential firing during GSWDs, which parallels earlier reports on cellular excitability and hypersynchronicity in thalamo-cortical networks in this model [36, 352, 437], and other rodent models of absence epilepsy [438]. Our single-cell recordings showed that ~50% of neurons recorded in primary, associative and intralaminar thalamic nuclei fire most of their action potentials ~20 ms prior to the peak of the ECoG spikes during GSWD episodes. In the other rodent models this delay in thalamo-cortical activity ranged from 9 ms in GAERS to 28 ms in Long-Evans rats [35, 99]. In contrast to a rather fixed periodicity in thalamic firing, cerebellar firing is known to be far more variable when compared to cortical GSWDs [46, 104, 439]. Although it is not known whether CN neurons show increased levels of synchrony during GSWDs and thus could contribute to driving synchronous thalamic firing [123, 124], our findings indicate that CN output has a rather opposite effect: synchronizing CN firing by direct CN stimulation desynchronizes thalamic firing. Our previous pharmacological interventions confirm this anti-seizure effect of cerebellar output, and showed that GSWD occurrence was prevented by enhancing CN firing, whereas dampening of CN action potential firing strongly increased the seizure load [46]. Also in refractory epilepsy dentate CN stimulation has such dual effect, which was recognized to have therapeutic value [12, 48, 49].

Increasing cerebellar output resulted in a variable effect on thalamic nuclei. Anatomical connections between cerebellum and thalamus and the impact on cerebral cortical activity revealed that in various species CN axonal projections to VL neurons and the interconnected motor cortex are excitatory [84, 89-92, 363, 364, 366, 380, 387, 399, 440, 441]. However, early reports indicated bi-modal responses following electrical stimulation of the cerebellar nuclei in cats [92, 330, 389]. Although such responses may be easily caused by intra-thalamic inhibitory projections that run through the reticular thalamic nucleus, we speculate that axonal connections from CN to other pre-thalamic nuclei, such as the middle and deeper layers of the superior colliculus, the zona incerta and the anterior pretectal nucleus, contribute to the differential thalamic responses to CN stimulation (see also [430, 442]. Other sources that could contribute to a desynchronizing effect of CN stimulation on thalamic firing come from: *i*) inhibitory afferents that manipulate thalamic responses [443] to CN stimulation, as has been shown for substantia nigra pars reticulata input to VM neurons [421]; *ii*) an increased contribution of $Ca_V2.2$ (N-type) voltage-gated Ca^{2+} channels to neurotransmitter release to compensate the loss of $Ca_V2.1$ (P/Q-type) channel function in *tottering* mice, which may increase the asynchronous release of neurotransmitter (as discussed by [444]); *iii*) excitation of pre-motor CN that do not project to the thalamus but rather to premotor nuclei in the brainstem and thereby drive behavioral motor responses [111]; such behavioral responses are likely to affect thalamo-cortical synchrony through the coding of proprioceptive input (see for instance ref [445]).

In conclusion, our data show that targeted stimulation of CN neurons results in desynchronization of thalamic firing in line with termination of GSWDs in *tottering* mice. We thereby suggest CN as an important node in the neuronal network underlying generalized seizures. Stimulating this node can not only acutely stop hypersynchrony in the thalamo-cortical networks during seizures, but may also have more general effects. For example, cerebellar output has been implicated in cognitive processes, like social interaction [385, 386], sensory coding [90, 387], and language [446], all of which have also been linked to the integrity of the thalamic structure and its activity [447]. Therefore, we argue that cerebellar stimulation may also have important effects on cognitive functioning in epilepsy patients (as reviewed by [448]).